SOCIETY FOR SCIENCE AND EDUCATION
UNITED KINGDOM
TMLAI TRANSACTIONS ON MACHINE LEARNING AND ARTIFICIAL INTELLIGENCE
ISSN 2054-7390

Robot-Server Architecture for Optimizing Solar Panel Power Output

Ernesto Zamora Ramos, Maria Ramos, Konstantinos Moutafis and Evangelos A. Yfantis
University of Nevada, Las Vegas, Nevada, 89154, USA
zamorara@unlv.nevada.edu, ramosm27@unlv.nevada.edu, moutaf@gmail.com, yfantis@cs.unlv.edu

ABSTRACT

Solar panel facilities for generating electricity have increased exponentially in the recent years. Dust and bird droppings on the solar panels inhibit the energy production. Having people to inspect them and, if needed, clean them is expensive and increases the energy cost. In this research paper we introduce a robot-server architecture for the purpose of inspecting the panels and cleaning them if there is a need for it. The general architecture of the robot consists of a mechanical part, an electromechanical part, an electronic part, and a software part. The mechanical and electromechanical parts consist of an all-terrain vehicle, two electric brushless motors, a telescopic vision system, and telescopic cleaning system with a brush, stepper motors controlling the telescopic vision system, and the telescopic vacuum system with a brushless electric motor. The electronic system consists of three electronic speed controllers, navigation sensors, a computer board, a hard disk, a transceiver, and an antenna for wireless communication. The software consists of a scalable operating system, an intelligent vision system with pattern recognition, a communication software system, an intelligent navigation system, and a file server with a database, TLS security, network communication software based on UDP, and internet communication based on websockets and TCP-IP. In addition to that for street solar lights we designed a PCB board with a sensor that activates a mechanism similar to windshield wipers that cleans the glass of the solar panels powering the lights automatically when needed.

Keywords: Robotic Vision, Solar Power Optimization, Pattern Analysis, Autonomous Vehicles.

1 Introduction

The energy produced by solar panels keeps increasing yearly. Silicon solar panels produce by Panasonic have 22.8% efficiency, making solar panels an economically viable alternative to traditional power. Companies like First Solar it has converted 22.1% of the sunlight energy into electricity using experimental cells made from cadmium telluride. New semiconductor technologies based on Gallium Arsenide and Indium Gallium Nitride (inGan) promise a major improvement over silicon solar panels. Also multi-junction solar panels have higher production of electric energy. Gallium nitride Solar panels are relatively inexpensive, they last for a considerable amount of time, and every year we see new large scale installations as well as smaller for houses and commercial buildings. Many of these large scale installations are in desert environments, where strong winds blow sand and dust onto the panels inhibiting the energy productions. In addition to that birds migrating from colder to warmer climates choose the solar panel sites as a resting place and the bird droppings on the panels inhibit the energy production. Also small

DOI: 10.14738/tmlai.44.2141
Publication Date: 18th August, 2016
URL: http://dx.doi.org/10.14738/tmlai.44.2141

animals with sharp teeth roaming on the solar panel site at night, or using the space under the panels to protect themselves from the hot summer days and the cold winter nights cut the cables with their sharp teeth thus disabling the panels. Finally vandals throwing stones and other objects through the fence could damage the glass or other parts of the panels.

Having a maintenance crew to look after the panels is an expensive proposition which introduces human problems.

Here we introduce a robot that we named "Helios." Its purpose is to inspect every panel, as well as its cable connections, and decide if the panel needs cleaning or not.

All the pertinent information, which includes the panel id, and the details related to the panel status are transmitted wireless to a file server and stored in the data base. For each panel needed cleaning the robot returns during the night when the panel does not produce any energy and cleans the panel using the brush and the vacuum.

The robot (figure 1), consists of a mechanical part, an electromechanical part, an electronics part, and a software part.

The mechanical and electromechanical parts consist of an all-terrain vehicle, two electric brushless motors, a telescopic vision system, and telescopic cleaning system with a brush, stepper motors controlling the telescopic vision system, and the telescopic vacuum system, and a small vacuum system with a brushless electric motor. The vacuum system traces the solar panel from top to bottom and cleans it.

Figure 1: Prototype of the robot Helios with the folding telescopic support of the vision system consisting of four cameras and a noninvasive laser.

The electronics system consists of three electronic speed controllers, a number of ultrasound sensors, navigation sensors, a computer board, a hard disk, a transceiver, and an antenna for wireless communications.

The software consists of a scalable operating system, an intelligent vision system with pattern recognition, a communication software system, and an intelligent navigation system.

The computer mother board has a solid state high capacity hard disc to store the operating system, with several gigabytes of memory, a light SQL database with the location of each panel and other panel

information. The wireless communication system includes a transceiver, an antenna, an MCU, and memory, and a network software system for communication with the file server. The file server contains the database holding information about each panel, and about each robot.

In this research paper we describe the general architecture of the robot, which includes the mechanical design, electronics and software architecture. This research paper is structured as follows: The abstract is followed by the introduction which is followed by the background information, which is followed by the Robot-server architecture, ending with the conclusion, and the references.

2 Background information

Renewable energy represents a large number of energy solutions promising to replace or reduce the dependency of energy sources of the past that are not friendly to the environment, and are limited so in the future we run the risk to run out of these resources. As more emphasis is placed to research and development of new renewable energy technologies that are more efficient, cost effective, and non-environmentally toxic to provide energy for our energy needs in our houses, business, street lights, public buildings, transportation, communications, and help create clean smart cities with cleaner air, that provide a healthier environment.

Photogrammetry (photo-light, gram-drawing, metry-measuring) has a Greek derivation, and is the practice of determining the geometric properties of objects from photographic images. It is dated back to nineteenth century when film photography started. The process is as simple as getting the distance between two points on a plane parallel to the photographic image plane. Work in stereo photogrammetric image enhancement, image processing, and stereo vision started in the later part of the last century.

Our work pertains to robot-server communication, specialized robot architectures, robot vision, machine intelligence and pattern recognition [1-8], robot navigation, and autonomous machines.

The vision system used in our robot system consists of four cameras on a cross framework. The horizontal and vertical dimensions of the cross at the default state are equal. The cross has telescopic components so that the cameras could be at different distances from the center. In the center of the cross there is a non-invasive laser. The cross is supported by a mechanism that allows the system of four cameras to pan and tilt. Each camera is supported by its own pan and tilt mechanism. The Mathematics and analytics of the computer vision system are presented in this research as well as the architecture of the robot.

3 The Robot-Server Architecture

The Robot-Server architecture is very similar to the server-client paradigm. The server has a data base that includes each robot, each panel, and the pathway to each panel, from an origin. The server also includes the local area network of the server and robots, the communication software between the server and each robot. The robots include the image processing, classification, and the software driving the robot, and enabling the robot to perform cleaning, and other functions. The majority of the effort is in the software, making the robot to be a specialized computer on wheels. The hardware consists of three parts.

3.1 The Mechanical Component

The mechanical component comprises the vehicle which is an all-terrain using an army-tank-like continuous track, with two brushless motors, one in each front wheel. Each one of the motors is controlled by a separate electronic speed controller. The main reason for this is to enable the robot to make turns. Thus in order for the robot to turn left; we increase the speed on the right motor and decrease the speed

on the left. The mechanical part also includes a telescopic vision system which provides the input to the intelligent software that understands a panel's boundaries and decides if a panel is clean or needs to be cleaned. The mechanical part also includes the vacuum and a brush used to loosen material on the panel in order for the vacuum to clean the panel.

The electromechanical system includes the two brushless motors of the vehicle part of the robot, the stepper motors of the telescopic vision system, as well as the stepper motors of the telescopic vacuum system, and the brushless motor of the vacuum system.

3.2 The Electronic Component

The electronic part consists of a printed circuit board (PCB) connected to the four cameras via four BNC connections, having a number of sensors used as part of the navigation system, GPS, accelerometer, magnetometer, a DSP that takes as input the images obtained by the four cameras via the BNC connections, stores the images in four memory chips on board, performs the classification algorithm and makes a decision if the panel is clean or needs cleaning. The decision is passed to the transceiver on board to transmit it wireless to the file server. The PCB board also contains a control system that uses an ARM chip to compress the images obtained by the four cameras, passes them to the transceiver on board which transmits them to the file server; a transceiver, a voltage amplifier that amplifies the voltage from 1.5V to 12V, and an antenna. The PCB board is connected to a computer board via a PCI express connection.

3.3 The Vision System

The software consists of the classification algorithm, that takes as input the images of the panel obtained by the four cameras, applies the classification algorithm and decides if the panel needs cleaning. The vision system also inspects the electric cables underneath the panel and decides if all connections are good or not.

The vision system is part of the robot and it consists of four identical cameras and a non-invasive laser. Figure 2, depicts the schematics of our system. The cameras are mounted on a frame having a cross configuration. Each leg of the cross is telescopic having the ability to increase or decrease the distance of the camera from the laser so that will decrease or eliminate occlusions. The distance of each camera from the center of the cross is controlled by a stepper motor and it is always known. The noninvasive laser is in the middle of the cross and is equidistant to the four cameras. When distances are to be resolved the noninvasive laser is activated and its light is registered by each one of the four cameras. The cameras are parallel to one another and also parallel to the laser. During calibration for every pixel in the image space registering the laser light dot on the object, the angle between the line defined by the image center and the pixel, and the line defined by the pixel and the laser dot on the object, is computed and stored in a lookup table. Thus during the focus on a panel if for a camera the laser dot is registered by a certain pixel then we know the angle formed by the line between the pixel and the laser dot and the line between the pixel and the camera center.

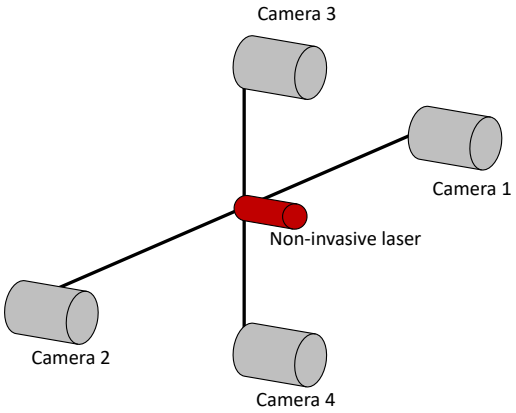

Figure 2: The schematics of our vision system. The vision system consists of four identical cameras and a noninvasive laser. The purpose of the system is to resolve distances, and enable the creation of 3-D vision.

Figure 3 shows each of the four cameras with each own local coordinate system. In the default state the laser and the cameras are parallel and the distance of each camera from the laser is fixed. The default state is the one we use in order to position the camera system at a fixed distance from the panel. In this state the laser dot has exactly the same *Z* coordinate for each one of the four local camera coordinate systems.

The *Z* coordinate for a pinhole camera (figure 4), is given by equation 1. If *B* is the known distance between the focal points of cameras 1 and 2 then equation 4 gives an estimate of the distance of the laser focal point to the laser dot on the panel. In a similar way we can obtain another estimate of *Z* from the cameras 3 and 4. Two estimates of *Z* can be obtained from cameras 1 and 3, another two from cameras 2 and 3, another two estimates of *Z* from cameras 1 and 4, and finally another two estimates of *Z* from cameras 2 and 4. An estimate of *Z* can be obtained from camera 1 and the laser, similarly another from camera 2 and the laser, from camera 3 and the laser, and from camera 4 and the laser.

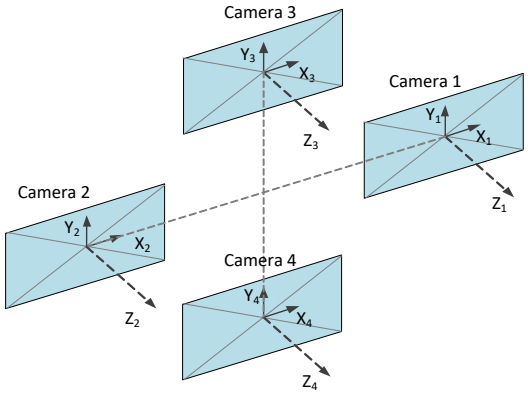

Figure 3: Each one of the cameras has a local coordinate system (X_i, Y_i, Z_i), and an image space coordinate system (x_i, y_i), $i \in \{1,2,3,4\}$. The local coordinates can easily be transformed to a global coordinate system via translation and rotation.

Thus, 14 estimates of the distance of the laser focal point from the laser dot on the panel can be obtained. All these estimates are slightly different due to the noise in the system. The average $\overline{Z}$ of these fourteen estimates is a more accurate estimate of the distance of the vision system from the panel. The DSP of the

PCB board computes this distance relatively fast and positions the vision system at a fixed distance above the panel. This distance is the same at every inspection of every panel. The details of the geometry and formulas are given below.

The pinhole camera model can also represent the modern CCD or CMOS cameras with the chip replacing the film and the center of the lens replacing the pinhole. In figure 4, *O* is the center pixel of the imager chip, and also the center of the local coordinate system. $L(0,0,f)$ is the lens center, $P(X,Y,Z)$ is a point in the space projected to the point $\hat{P}(x,y)$ on the imager. Then from the similar triangles ΔALB and ΔOaL, if $\lambda = \overline{LO}$, $\overline{Oa} = x$, $\overline{LB} = Z - \lambda$, we have:

$$-\frac{Z-\lambda}{\lambda} = \frac{X}{x}, \text{ or } Z = \lambda\left(1 - \frac{X}{x}\right) \tag{1}$$

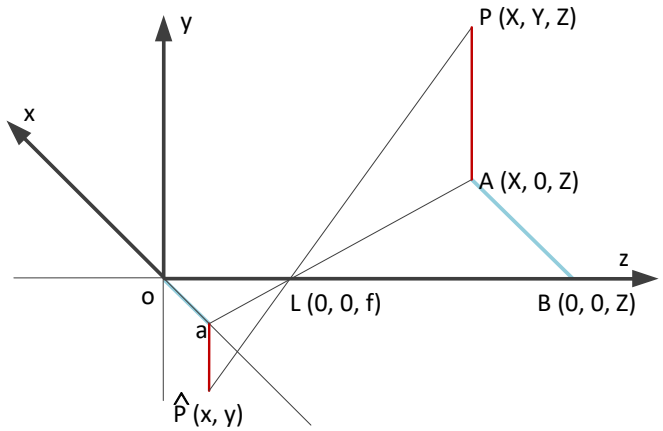

Figure 4: Pinhole camera model. L is the camera pinhole or the center of the lens. *O* is the center of the imager, as well as the origin of the local coordinate system (X,Y,Z), and the image coordinate system (x,y). The point $P(X,Y,Z)$ is projected to the point $\hat{P}(x,y)$.

From equation 1 we have:

$$Z = \lambda\left(1 - \frac{X_1}{x_1}\right) \tag{2}$$

$$Z = \lambda\left(1 - \frac{X_2}{x_2}\right) = \lambda\left(1 - \frac{X_1 + B}{x_2}\right) \tag{3}$$

Thus from 2 and 3 we get:

$$Z = \lambda\left(1 - \frac{B}{x_2 - x_1}\right) \tag{4}$$

Due to the noise in the system we obtain four different estimates of *Z* from the four laser-camera geometries: two estimates using the geometry of two horizontal and two vertical cameras. Eight different estimates of *Z* can be also obtained using the geometry of any two adjacent cameras. Each one of these estimates is a random variable with mean Z_t, the true value of the distance, and variance σ_i^2, $i \in \{1,2,...,14\}$. According to the central limit theorem the average $\bar{Z}$ of these estimates of the distance is normally distributed with mean Z_t, where Z_t is the true distance, and variance

$$\sigma_{\bar{Z}}^2 = \frac{\sum_{i=1}^{14} \sigma_i^2}{14}.$$

Let S_Z be an estimate of the standard deviation of the random variable *Z* based on the estimates of the true distance, and if we denote by Z_t the true value of *Z* then the statistic:

$$\frac{\bar{Z} - Z_t}{\frac{S_Z}{\sqrt{14}}}$$

has the *t* distribution with 13 degrees of freedom. Therefore

$$\bar{Z} - t_{1-\frac{\alpha}{2},13} < Z_t < \bar{Z} + t_{1-\frac{\alpha}{2},13} \tag{5}$$

with probability $1-\alpha$

Formula 5 provides a measure of how accurate the distances estimated by our system are. For example if $\bar{Z} = 100\text{cm}$ and $S_Z = 3\text{cm}$, then with probability 0.95 (95%) the true distance Z_t, is $98.27\text{cm} < Z_t < 101.73\text{cm}$.

4 Experimental Results

As the robot prototype is still in development, we have directed experimentation and evaluation to testing completed components of the software and hardware.

Table 1 Results of equation 6 from applying Jackknife test on all three groups of sample data [1].

Group	TN	FN	TP	FP	Accuracy (%)	Misclassification Error
1	12	0	12	0	100	0
2	17	3	19	1	90	0.10
3	17	2	19	0	94.4	0.0526

The energy produced by solar panels declines in proportion to the amount of light blocked by the deposits of dust and other contaminants accumulating on the surface of the photovoltaic cells.

Our current work regarding the classification system employed by the robot to determine if a panel is clean or not is based on the Mahalanobis distance, which is the relative, statistical measure of the data

point's distance from a common point. The classifier we developed for the system recognizes the state of the panel with accuracy above 90%.

To evaluate the accuracy of the classification system we obtained sample images from solar panels using a camera configuration similar to what will be part of the finalized vision system of the robot. We decided to employ three groups of training data, where each group contains one clean sample set and one dirty sample set.

1) The first group contains data from the same panel.
2) The second group builds upon the first group by incorporating data from another panel with similar photovoltaic cell structure.
3) The third group does not build upon the first and second group. Instead, it incorporates data from two panels of similar characteristics, but with a lighter shade of blue than the panels from the other groups.

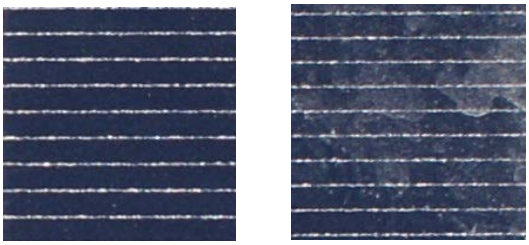

Figure 5: Solar panel samples: left) clean panel; right) dirty panel [1].

See figure 5 for two samples taken by the vision system of clean and dirty solar panels.

Then we utilized the jackknifing technique to estimate the precision of the classifier through the formula:

$$Accuracy = \frac{TN + TP}{TN + TP + FN + FP} \tag{6}$$

where TN (true negative)/FN (false negative) are the number of samples correctly/incorrectly classified as clean, and TP (true positive)/FP (false positive) are the number of samples correctly/incorrectly classified as dirty [1].

Table 1 shows the experimental results obtained from the sample data.

Further development, experimentation and evaluation of other components are still in progress for this project. The results of the vision system are, however, very promising.

5 Conclusion

In this research paper we describe the architecture of a Robot-file server system still in experimental and development form, used to recognize if solar panels are dirty and lose energy above a critical value. In such cases, the robot cleans the affected panels and transmits this information to the file server in order to update the flag on record related to the panel in the database to "cleaned" along with the date it was cleaned.

The robot software includes a scalable operating system, along with an intelligent navigation system, classification software, software driving the cleaning mechanism, and communication software that include web socket communication, and network socket communication.

ACKNOWLEDGEMENT

This Research was supported by the National Science Foundation (NSF) Nexus of Food, Energy and Water grant No. IIA-1301726.

REFERENCES

[1]. E. Zamora Ramos, S. Ho, and E. A. Yfantis, *Using spectral decomposition to detect dirty solar panels and minimize the impact on energy production.* Journal of Advances in Image and Video Processing, 2015. 3(6): p. 1-12.

[2]. E. A. Yfantis, *Telemedicine: The present and its future.* In *Plenary Lecture: 14th International Conference in Applied Computer Science.*

[3]. E. A. Yfantis, *Dynamic redundancy bit allocation and packet size to increase throughput in noisy real time video wireless transmission.* The Journal of Combinatorial Mathematics and Combinatorial Computing JCMCC 86, 2013. p. 163-169.

[4]. E. A. Yfantis et al, *Pollution detection in urban areas using the existing camera networks.* International Journal of Multimedia Technology, 2013. 3(3): p. 98-102.

[5]. E. A. Yfantis and A. Fayed, *Authentication and secure robot communication.* International Journal of Advanced Robotic Systems, 2014. 11: p. 1-6.

[6]. E. A. Yfantis and A. Fayed, *A camera system for detecting dust and other deposits on solar panels.* Journal of Advances in Image and Video Processing, 2014. 2(5): p. 1-10.

[7]. E. A. Yfantis and A. Fayed, *Robot vision and distance estimation.* In *14th International Conference in Applied Computer Science*, Cambridge, MA, Jan 2014. p. 215-220.

[8]. E. Zamora Ramos et al. *A Robot Architecture for Detecting Dust and Cleaning Solar Panels*. In *31st International Conference on Computers and Their Applications, CATA 16*, Las V